AFRL-RY-WP-TR-2011-1314

MULTICAST PARAMETRIC SYNCHRONOUS SAMPLING

Stojan Radic

University of California San Diego

SEPTEMBER 2011
Final Report

AIR FORCE RESEARCH LABORATORY
SENSORS DIRECTORATE
WRIGHT-PATTERSON AIR FORCE BASE, OH 45433-7320
AIR FORCE MATERIEL COMMAND
UNITED STATES AIR FORCE

NOTICE AND SIGNATURE PAGE

Using Government drawings, specifications, or other data included in this document for any purpose other than Government procurement does not in any way obligate the U.S. Government. The fact that the Government formulated or supplied the drawings, specifications, or other data does not license the holder or any other person or corporation; or convey any rights or permission to manufacture, use, or sell any patented invention that may relate to them.

This report was cleared for public release by the USAF 88th Air Base Wing (88ABW) Public Affairs Office (PAO) and is available to the general public, including foreign nationals. Copies may be obtained from the Defense Technical Information Center (DTIC) (http://www.dtic.mil).

AFRL-RY-WP-TR-2011-1314 HAS BEEN REVIEWED AND IS APPROVED FOR PUBLICATION IN ACCORDANCE WITH ASSIGNED DISTRIBUTION STATEMENT.

*//Signature//

KENNETH L. SCHEPLER
Laser Sources Section
EO CM Tech Branch
Multispectral Sensing & Detection Division
Sensors Directorate

//Signature//

JOHN F. CARR, Chief
EO CM Tech Branch
Multispectral Sensing & Detection Division
Sensors Directorate

//Signature//

WILLIAM MITCHELL, Chief
Laser Sources Section
EO CM Tech Branch
Multispectral Sensing & Detection Division
Sensors Directorate

//Signature//

TRACY W. JOHNSTON, Chief
Multispectral Sensing & Detection Division
Sensors Directorate

This report is published in the interest of scientific and technical information exchange, and its publication does not constitute the Government's approval or disapproval of its ideas or findings.

*Disseminated copies will show "//Signature//" stamped or typed above the signature blocks.

REPORT DOCUMENTATION PAGE

Form Approved
OMB No. 0704-0188

1. REPORT DATE *(DD-MM-YY)*	2. REPORT TYPE	3. DATES COVERED *(From - To)*
September 2011	Final	01 March 2008 – 30 September 2011

4. TITLE AND SUBTITLE
MULTICAST PARAMETRIC SYNCHRONOUS SAMPLING

5a. CONTRACT NUMBER
FA8650-08-1-7819

5b. GRANT NUMBER

5c. PROGRAM ELEMENT NUMBER
62716E/62204F

6. AUTHOR(S)
Stojan Radic

5d. PROJECT NUMBER
ARPR

5e. TASK NUMBER
YJ

5f. WORK UNIT NUMBER
ARPRYJ00

7. PERFORMING ORGANIZATION NAME(S) AND ADDRESS(ES)
University of California San Diego
Electrical and Computer Engineering
9500 Gilman Drive
La Jolla, CA 92093-0407

8. PERFORMING ORGANIZATION REPORT NUMBER

9. SPONSORING/MONITORING AGENCY NAME(S) AND ADDRESS(ES)
Air Force Research Laboratory
Sensors Directorate
Wright-Patterson Air Force Base, OH 45433-7320
Air Force Materiel Command
United States Air Force

Defense Advanced Research Projects Agency/Microsystems Technology Office (DARPA/MTO)
3701 N. Fairfax Drive
Arlington, VA 22203-1714

10. SPONSORING/MONITORING AGENCY ACRONYM(S)
DARPA and AFRL/RYMWA

11. SPONSORING/MONITORING AGENCY REPORT NUMBER(S)
AFRL-RY-WP-TR-2011-1314

12. DISTRIBUTION/AVAILABILITY STATEMENT
Approved for public release; distribution unlimited.

13. SUPPLEMENTARY NOTES
PAO Case Number: 88ABW-11-5835, cleared 04 Nov 2011. This report contains color.

14. ABSTRACT
Parametric signal processing technology is described. Work on mixer synthesis, gain and conversion efficiency, signal multicasting and sampling is outlined in detail. The technology limits and its applications in multiplexing, demultiplexing, amplification, conversion and signal delay construction are described. Achievements include (i) longitudinal nonlinear waveguide characterization which resulted in unprecedented mixers surpassing 20 THz in bandwidth and > 20 dB gain, (ii) ability to copy THz signals with impunity to tens of replicas; (iii) all-optical delays > 1.9 us; (iv) 10's of THz-fast all-optical sampling of signals and (v) an original fully scalable MPASS parametric processor for detection of THz signals availing access to all the (ultra high speed) data all the time at 640 Gbps over 100 km transmission distance.

15. SUBJECT TERMS
telecommunications, parametric processing, amplification, mixer construction, four-photon mixing

16. SECURITY CLASSIFICATION OF:			17. LIMITATION OF ABSTRACT:	18. NUMBER OF PAGES	19a. NAME OF RESPONSIBLE PERSON (Monitor)
a. REPORT	b. ABSTRACT	c. THIS PAGE			Kenneth L. Schepler
Unclassified	Unclassified	Unclassified	SAR	34	19b. TELEPHONE NUMBER *(Include Area Code)* N/A

Table of Contents

List of Figures

Figure **Page**

Acknowledgement

This work was supported by the Air Force Research Laboratory (AFRL) and the Defense Advanced Research Agency (DARPA) under Grant/Cooperative Agreement No. FA8650-08-1-7819 entitled Parametric Optical Processes and Systems. We gratefully acknowledge the support and encouragement of Kenneth L. Schepler, Contracting Officer's Technical Representative (COTR).

1) Introduction

The Parametric Optical Processing and Systems (POPS) program was initiated within DARPA in recognition of a vast discrepancy between the ever rising information rates and bandwidths, on the one hand and the capabilities / tools of their real time analysis on the other. Indeed, as the aggregate transmission information capacities are slowly, but surely approaching THz bandwidth per single optical fiber, there are no tools currently available for their real time capture and analysis. More concretely, although an access to the stated information speeds is possible - e.g. by recording finite length segments which can be post-processed at a later time, before the POPS program initiation, there were no means that would avail access to a full data gamut, and more importantly not in a continuous time (or as is often referred to 'all the data all the time'). In particular, processing based on electronic circuits is currently some two orders of magnitude away from this target. The POPS program sought to approach this interface gap by means of optical parametric processing.

Parametric processes represent a particular class of nonlinear processes in which the frequency mixing (or, the mixing of photons of particular frequencies) strictly obeys energy and momentum conservation. In more detail, the described mixing occurs in a distributed fashion, as the (at least) two waves propagate through a nonlinear medium, such that new frequencies are generated. In addition to the nonlinear properties of the medium, the efficiency of this mixing is critically governed by the medium dispersive properties, whereas both the original and the newly generated frequencies need to travel synchronously. Indeed, any walk-off between the original and newly generated frequencies results in an energy flow redistribution, and thus to quenching of the conversion efficiency. In practice, the dispersion engineering of nonlinear waveguides is a mature field. However, waveguide fabrication is mired by finite precision resulting in dispersion fluctuations occurring at scales that seriously affect the energy exchange of the interacting waves, thus seriously limiting the mixer performance in practice. Therefore, it is really the dispersive properties that represent the critical component of the efficient mixer engineering. Although the underlying physics of the mixing processes is known, its implementation to practice obviously required devising new tools that would allow a highly accurate longitudinal characterization of mixer media, thus permitting a full-proof design and realization of uniform mixers with THz bandwidth.

With respect to the program goals, the PI and his Photonics Systems Laboratory at the University of California San Diego conceived an altogether innovative architecture in order to fulfill the program goals. In the very core of the concept lies a so-called Multicast Parametric Synchronous Sampling (MPASS) architecture shown in Fig. 1 [1]. The MPASS principle achieves a serial to parallel down-rating of high speed signals of arbitrary rates. It consists of (i) a multicasting part in which the incoming high speed signal is replicated to N replicas that reside on N distinct (carrier) wavelengths; (ii) delay (i.e. the time shift) part, which offsets the replicas in time by a precise amount, corresponding to the inverse of the following sampling gate repetition rate (R); and (iii) sampling in which the time-offset signal replicas are all sampled in parallel (i.e. by a single gate), whereas the subsequent wavelength demultiplexing allows a continuous access to the samples that contain all the relevant information for the signal reconstruction. More importantly all of the three major parts of the MPASS construct directly employ parametric physics to result in a single step, continuous access to arbitrarily high speed information. The additional salient feature of the MPASS architecture is that it is fully scalable in that the output

sampling rate is a product of the number of replicas (N), or the employed parallelism, and the sampling rate (R) of the parametric sampler in the last stage of the MPASS processor.

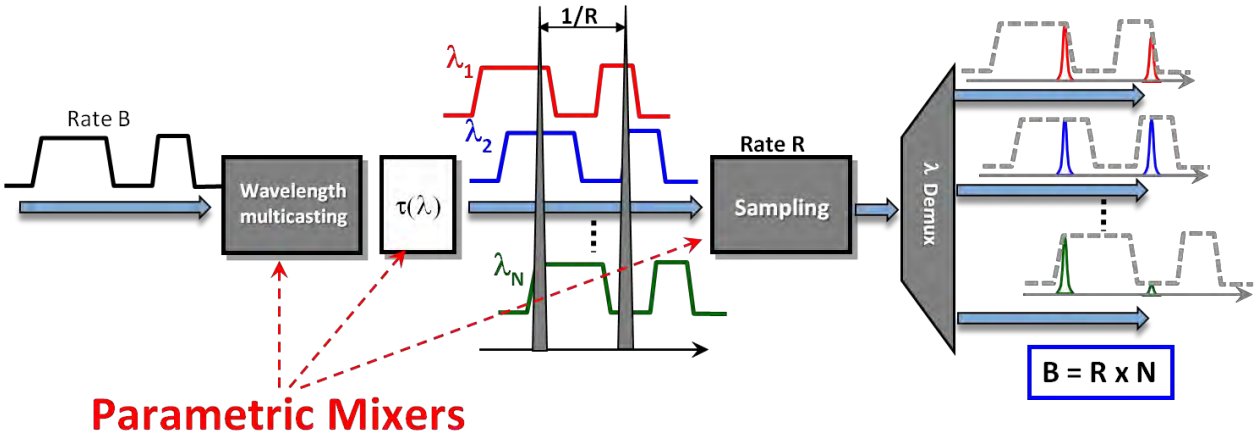

Figure 1. Multicast Parametric Synchronous Sampling (MPASS) architecture: A high data-rate signal, entering the MPASS block is multicast (i.e. replicated to N different wavelengths that are subsequently mutually delayed by exactly the period of the subsequent sampling block); all of the multicast copies are next simultaneously sampled in a multiwavelength sampling block, after which the subrate samples, pertinent to the multicast wavelengths are wavelength division multiplexed. The aggregate sampling rate is defined by the product of the number of multicast replicas (N) and the sampling rate (R).

Although, according to a simplified description of the previous paragraph, the MPASS principle may appear straightforward, attaining the POPS goals required designing a means to attaining repeatable wide bandwidth mixers that did not exist before the inception of the program. In fact, prior to the POPS program initiation, mixer construction resorted to fortunate outcomes in which the attainable mixing bandwidths were enslaved by stochastic instabilities in the fabrication. Thus experimental demonstrations represented but a stream of sporadic accidental realizations pertinent to academic laboratories, or results of computer simulations that altogether neglected the reality of the fabrication process.

2) Parametric Bandwidth and Gain Synthesis:

Before the inception of the POPS program, the state of high speed processing was, at best, at an academic level. Although the high speed capabilities of optical processing have been taken for granted, their application was sporadic and enslaved by the random mixer properties, as dictated by the inherent imprecision of the fabrication process [2]. Therefore ability to design and fabricate wide-band mixers was recognized as the first critical step towards improving the state of the art of the field. As a corollary to this effort, a new technique for dispersion mapping was devised allowing, for the first time, meter (even centimeter) precise characterization of nonlinear waveguides, leading to a deterministic, repeatable mixer design [3-6]. The technique relies on a novel concept of nonlinear gating, and basically opens a whole new class of waveguide characterization methods (i.e. not pertinent solely to dispersion mapping). Two generations of the characterization technique are shown in Fig. 2.

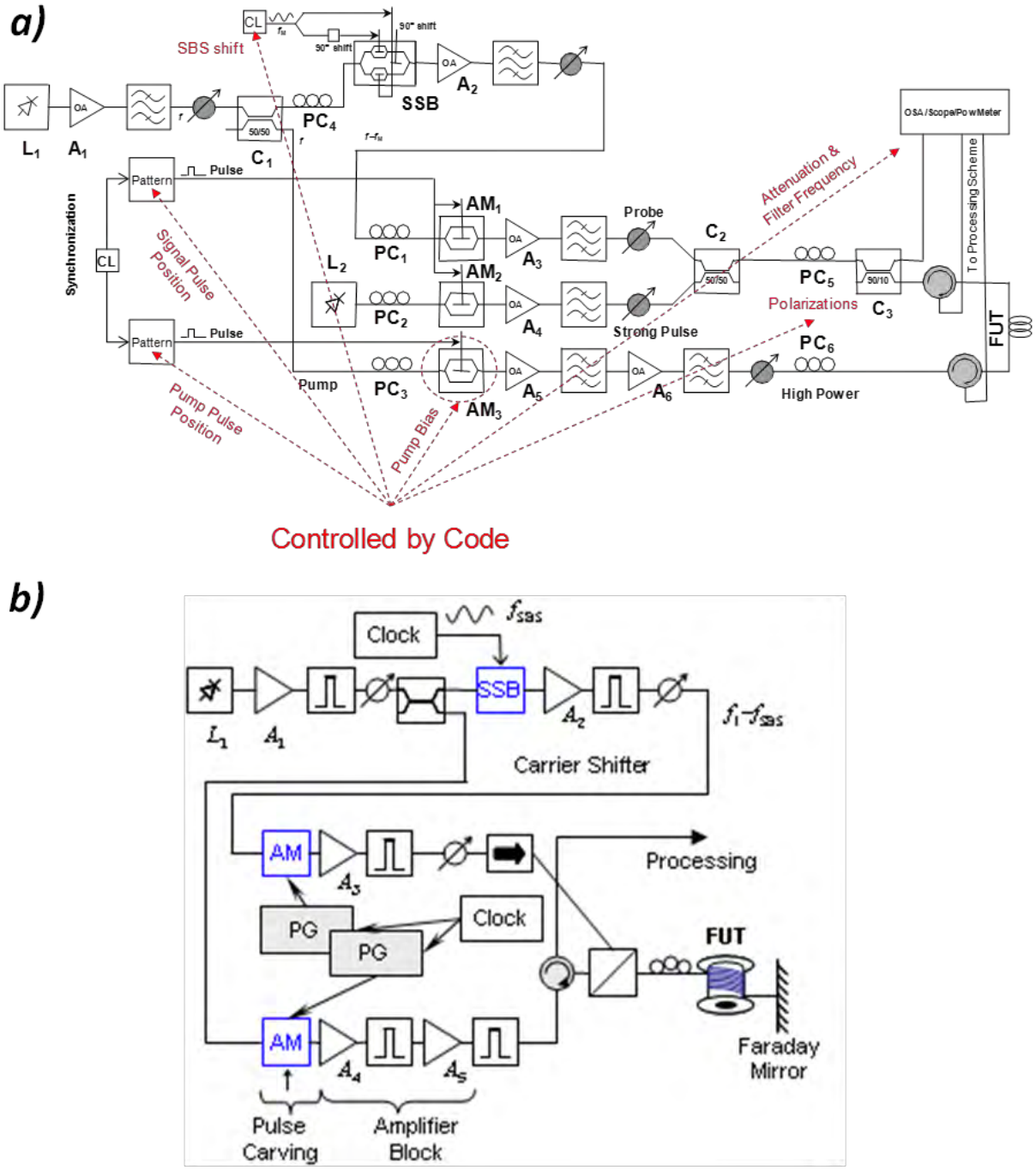

Figure 2. Setup schematics for the devised and developed nonlinear waveguide characterization technique. (a) first generation technique requiring full polarization tracking for all three waves; (b) second generation technique requiring no polarization tracking and resulting in a significant reduction in complexity.

The dispersion mapping technique, used in conjunction with dispersion trimming through precise waveguide straining, enabled a repeatable gain synthesis and the widest optical amplifiers produced to date [7,8]. Two prominent examples of synthesized gain are shown in Fig. 3.

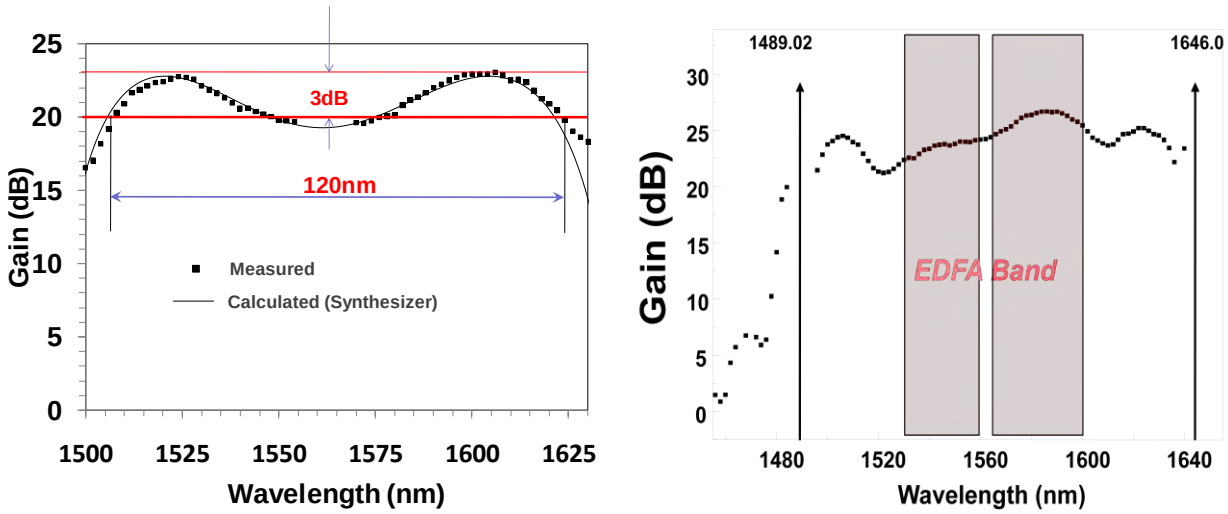

Figure 3. Deterministically synthesized and demonstrated parametric gain profiles, employing the dispersion mapping technique, with gain surpassing 20 dB over bandwidths surpassing 20 THz in a one-pump (left) and two-pump (right) realizations.

On the other hand, one of the main goals of the program set by the PI was a pursuit of diode-rated pump powers (i.e. pump powers up to 500 mW) in ultra efficient, ultra wide-band parametric devices. This target, considering the DARPA-hard POPS program goals directly translates into long interaction lengths, thus presenting extreme requirements on the dispersion mapping technique developed.

As will be shown in the remainder of this report this effort has proved to be more than well spent, as it has allowed realization of never before demonstrated ultra wide self-seeded interaction based on diode-pumped parametric mixers. The latter, in turn, proved to be the key enablers for a number of large-scale system demonstrations that will be described in the following.

3) Scalable Parametric Multicasting:

The ability to create a large number of signal replicas with impunity has been recognized as a key feature to MPASS architecture success. Indeed, the MPASS architecture heavily relies on the capability of parametric devices, with appropriate engineering and mixer design, to generate copies over 10-20 THz, as enabled by the dispersion mapping / gain synthesis described in the previous section. Although maturing through multiple stages and implementations, we provide a single, most prominent result in which the multicaster engineering has been pushed to its ultimate limits [9-12]. Motivated both to reach the program goal of using diode power limited parametric pumping, as well as answering the fundamental question on the attainable bandwidth, the number of copies over which a penalty-free multicasting can be performed, we have concentrated on the construction of a record performing multicaster, while at the same time determined to use severely constrained pump powers, thus forcing a steeply demanding task onto the mixer engineering and/or dispersion mapping techniques. Here we report on results, encompassing penalty free multicasting, and producing a record bandwidth-spanning optical frequency comb, relying on sub 500 mW pumping.

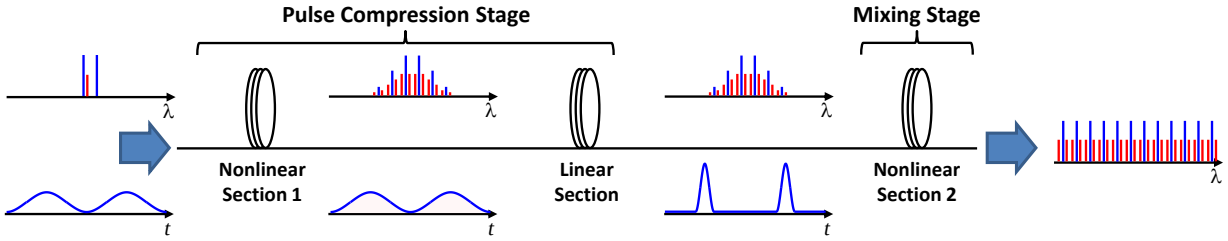

Figure 4. Principle of higher-order mixing enhancement in a parametric mixer device.

Fig. 4 shows the principle of generating uniform, high quality replicas extending over previously un-attainable bandwidths. In order to facilitate the description, let us first concentrate on the self-seeded higher order pump generation. In particular, the benefits of separating the self-seeding process into two steps have been recognized. As will be shown later, this assumption is proven crucial to the new concept of uniform wide-band self-seeding. The simultaneous containment of two tones in the spectral domain corresponds to a sinusoid (whose period is determined by the original tones' separation) in the time domain (Fig. 5(a)). In the previous statement we particularly concentrate on the two pronounced tones, as the two weaker sidebands are a consequence of nonlinear mixing inside the optical amplifiers. After having undergone mixing in a parametric medium (Fig. 5(b)), higher order harmonics are generated. In the time domain, the harmonics correspond to a more pulse-like shape (i.e. as opposed to a pure sinusoid at the very beginning) that becomes clearly discernible (see Fig. 5(a)). However, the harmonic generation is accompanied by frequency walk off due to the finite dispersion of the nonlinear medium that is equivalent to pulse spreading and to diminution of the peak power. It is, indeed, this peak power drop that limits the further self-seeded efficiency. From this perspective, however, the successful way further becomes self-suggestive: in order to sustain the efficient self-seeded multicasting, the peak power of the periodic waveform in the time domain needs to be restored by means of *dispersion compensation*. To facilitate the explanation, it is beneficial to revisit the time domain representation once more. The higher order generated harmonics that

make up the pulses in the time domain need to be brought to their transform limited shape, which is equivalent to enforcing a linear phase among the frequency components. The time and frequency domain illustrations are shown in Fig. 5 that, in fact, originate from an experimental characterization.

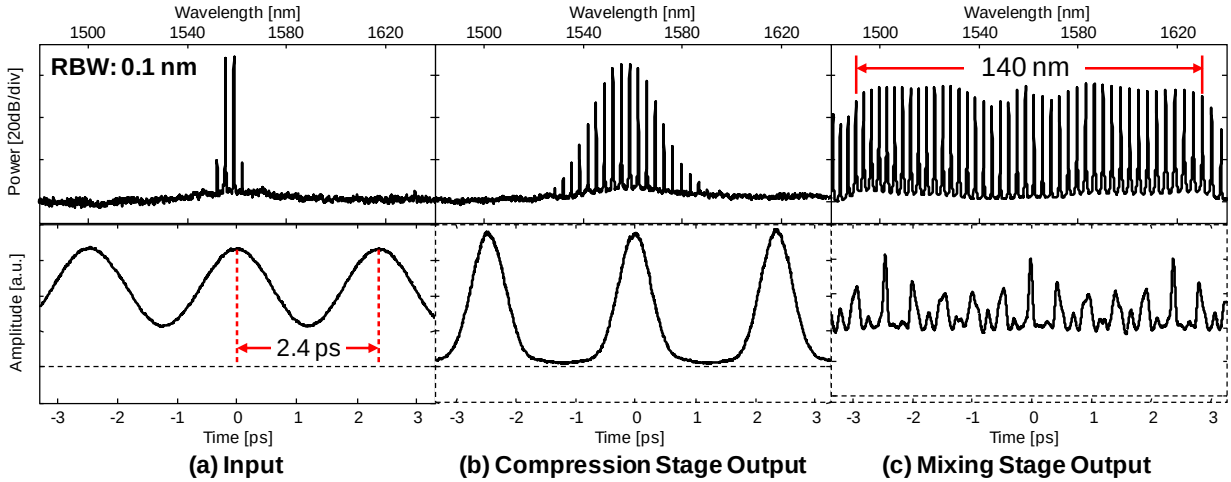

Figure 5. Optical spectra (top row) and auto-correlation traces (bottom row) of the pump field captured at various points in the multicasting mixer setup. Dashed lines in the lower plots indicate the ground-levels of the auto-correlation traces. RBW – resolution bandwidth.

After the linear compression, the phase aligned harmonics are launched into the second part of the nonlinear mixer. A careful study of the nonlinear interaction reveals the importance of the dispersion profile of the second nonlinear stage. In particular, we have determined parabolic dispersive shape to play the crucial role in the optimal expansion of the self-seeded generation. In particular, the benefits of the parabolic profile in this respect are two-fold: (i) the phase mismatch around the apex is significantly smaller than in the case of linear dispersion; (ii) the inherent dispersion symmetry of this profile straightforwardly ensures phase matching between the signal and idler pairs. Both of the stated reasons are highly beneficial for efficient cascaded four-wave mixing, which results in a far reaching uniform frequency comb generation. As implied in section 2, this effort required not only adaption of the longitudinal dispersion characterization to parabolic fibers, but also the adaption of dispersion tuning (e.g. through fiber stretching) in order to enable an optimal cascade formation. Fig. 5 shows the extent of 140 nm of exceedingly uniform frequency comb generated based on the principles described above.

Finally, to complete the multicasting task, if injected together with the first order pumps (as shown in the diagram in Fig. 4), a signal will be copied all along the span of the multicast pumps. In order to strictly quantify the multicasting performance, both intensity, and phase modulated signals were injected into the wide-bandwidth multicast setup. Fig. 6 shows the result of the rigorous quantification in terms of optical signal to noise ratio (OSNR) penalty with respect to the bit-error ratio (BER). Not only have all of the copies demonstrated error-less performance (60 of them), but some have outperformed the original signal (i.e. before multicasting).

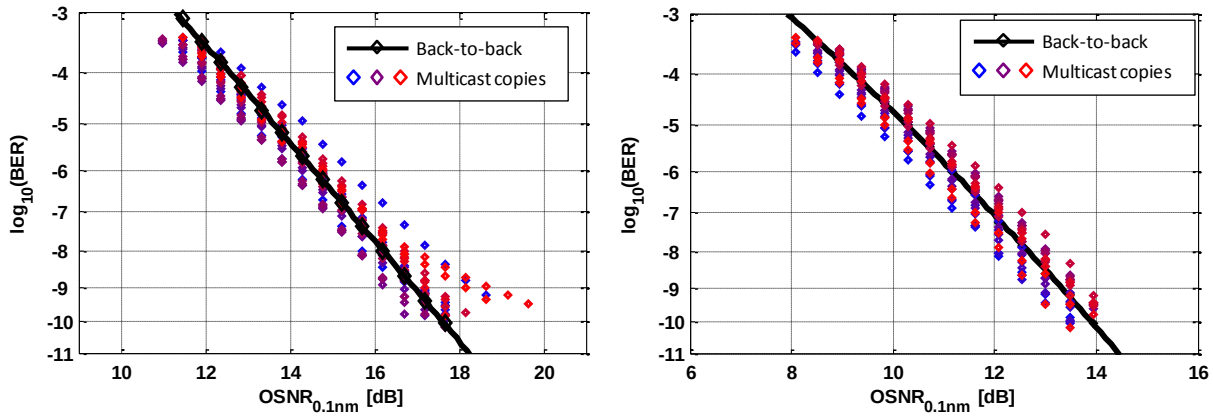

Figure 6. Ultra-wide bandwidth multicasting performance. (left) Intensity modulation multicasting. (right) Differential Binary Phase Shift Keying multicasting. Note that approximately one half of the multicast replicas exhibit performance superior to that of the original digital signal.

In summary, the described novel concept of ultra-wide band multicasting is the key element for (i) further advancement of the MPASS architecture capabilities; and (ii) ultra wide band optical combs. This previously unsuspected concept represents an outstandingly successful conclusion of the POPS program that was instigated by DARPA-hard challenging goals of the initiative.

4) Wideband Parametric Sampling

Parametric sampling represents the ultimate critical part of the MPASS architecture and is responsible for the direct and continuous acquisition of data across all of the multicast signal copies. Indeed, the ability to simultaneously sample high speed replicated signals has been performed in progression over the course of the program [1, 13-15]. Fig. 7 shows the schematic of the utilized principle. The pump pulsing was realized in terms of a cavity-less source that was developed as a part of the POPS program [16]. The cavity-less pulse source is derived from a continuous wave (CW) laser by a combination of chirping and pulse compression in an achromatic dispersive medium. In order to introduce the construction of the novel pulse source, note that optical pulses can be generated by carving a pulse from a (widely) tunable CW laser with an amplitude modulator driven by a harmonic radio-frequency (RF) source. Furthermore, in order to avail an efficient pulse duration control, the amplitude carver is followed by a phase modulator which imposes a phase shift under the pulse amplitude, resulting in strongly phase modulated (i.e. chirped) pulses. Subsequently, the pulses are temporally compressed by propagation in a dispersive medium, resulting in short optical pulses, as schematically shown in Fig. 8(b). A major advantage of a cavity-less pulse generation is that of obviating the need of feed-back control system, which makes it exceedingly robust and tolerant towards the environment perturbations. Finally, the timing jitter is determined solely by the underlying RF-source.

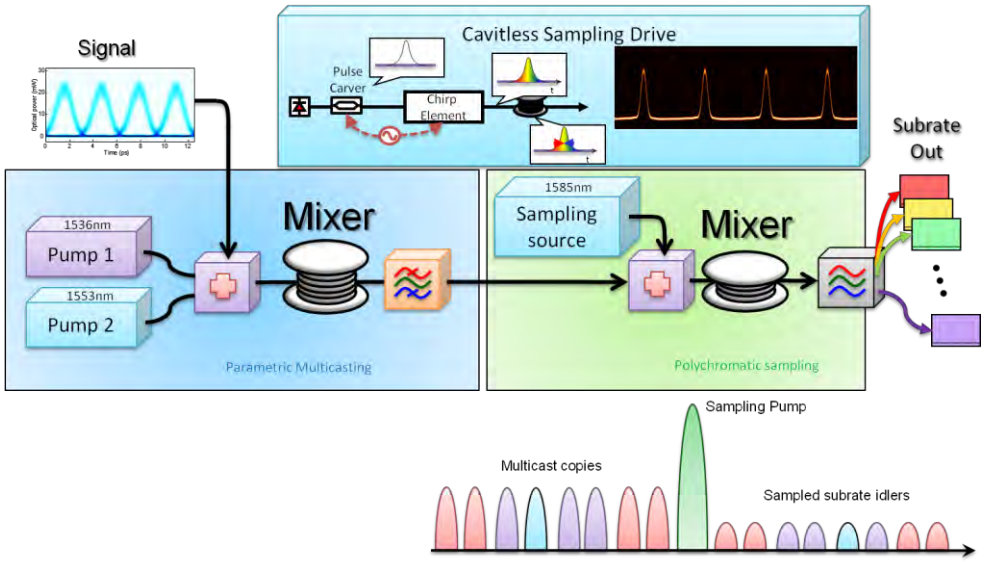

Figure 7. Wide band parametric sampling concept. Eight generated copies spanning 10's of THz generated through parametric multicasting are sampled simultaneously. Sampling is performed by means of the novel cavity-less source developed in the POPS program.

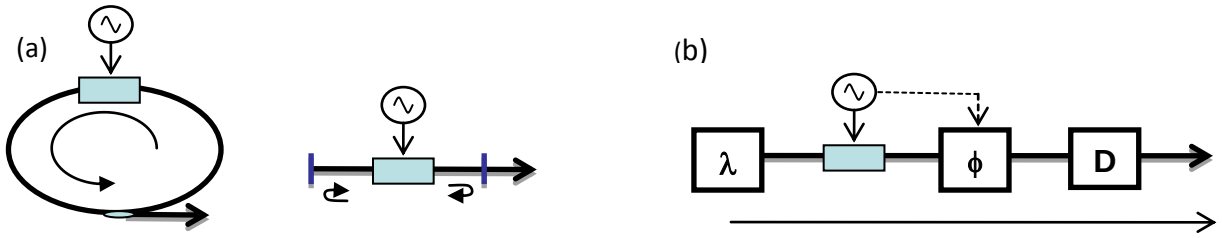

Figure 8. a) Pulses sources based on model locking in cavities. b) Pulse source based on the cavity-less principle with no cavity constraint.

In particular, the chirped pulses are generated by the concatenation of a Mach-Zehnder amplitude modulator (MZM) and a lithium niobate phase modulator (PM), both driven by a sinusoidal wave whose frequency determines the repetition rate of the pulse source. The CW light is first sent through the MZM. The MZM is biased below the quadrature point in order to generated pulses slightly shorter than half-period of the operating repetition rate as illustrated in Fig. 9. The pulses are subsequently frequency chirped in the phase modulator. The chirped pulses are finally compressed by dispersion in an optical fiber.

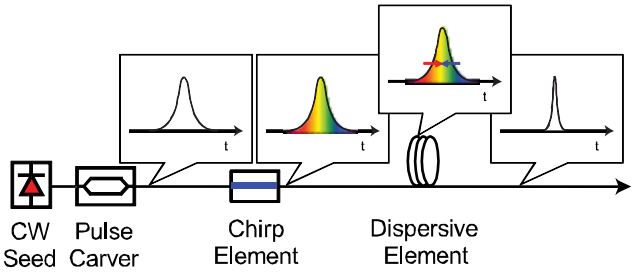

Figure 9. Principle of operation for the cavity-less pulse generation: Pulses are carved from CW light with a pulse carver and subsequently chirped with a chirp element and compressed in a dispersive element.

The sampling is performed in terms of a pulsed parametric amplifier, whereas all of the input signals (i.e. the multicast copies) are sliced and projected onto the corresponding idlers, at the instance of a short pulsed pump (see Fig. 1 for an intuitive explanation of the MPASS architecture). Moreover, each of the idler copies contains the full electric field information (of the corresponding signal) at the temporal instant of the pump. Fig. 10 shows the experimental result.

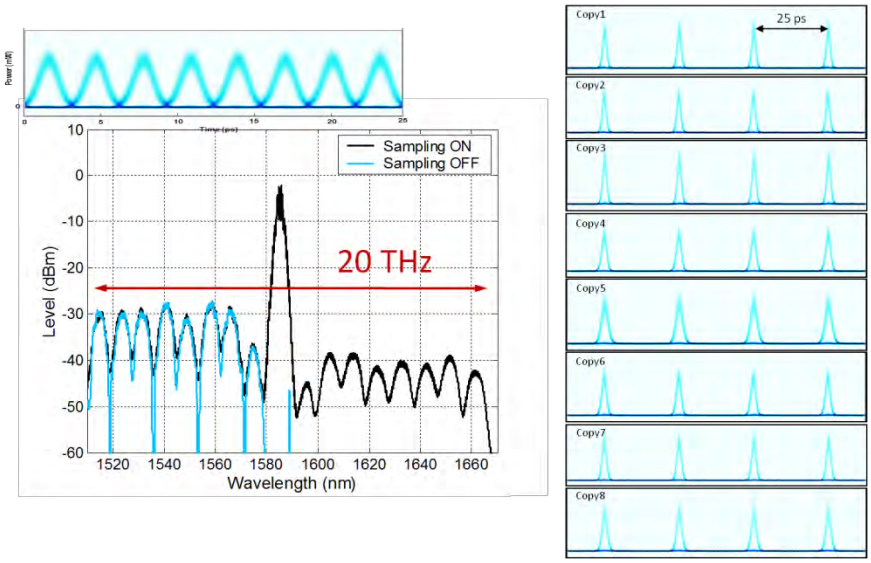

Figure 10. 20 THz Sampling gate. Eight copies are sampled simultaneously, while the corresponding 8 tributaries are demultiplexed to 8 different wavelengths in a single step, availing access to all-the-data-all-the-time.

As observed, a high speed data channel (320 Gb/s shown in Fig. 10) is successfully demultiplexed into 8 tributaries (shown on the right hand side of Fig. 10) in **a single step**. Indeed, the main strength of the MPASS architecture is that it significantly reduces the complexity of high speed signal manipulation. As a matter of fact, before the introduction of the MPASS architecture, as defined by the UCSD team, all-optical signal processing was performed on the 'per channel' basis, making it impractical for wide-spread exploitation. As clearly demonstrated in Fig. 10, aided by the capability to generate high quality wide bandwidth mixers, and with powerful copy-and-sample-all MPASS architecture, we were able to realize orders of magnitude complexity reduction, as well as the overall system performance that was just not possible before the POPS program.

In the remainder of this section, we shall concentrate on two advanced realizations that represent the state of the art of the field by furthering the MPASS concepts to a new technological level: Firstly, a new parametric clock recovery and tracking concept will be presented, and secondly a full scale self-tracked 640 Gb/s receiver, that was realized, will be described as well. The parametric clock recovery is based on the concept showed in Fig. 11 [17]. The novel parametric signal tracking gate is driven by a high-power pulsed source (pump) which generates pulses with temporal width comparable to the input signal pulses. Co-propagation of a signal and a pump pulse in a nonlinear fiber waveguide results in an idler pulse generation through the four-wave mixing (FWM) process. In the absence of a perfect pump-signal pulse synchronization, the pump pulse induces an XPM-mediated asymmetric spectral broadening (sometimes referred to as a shift) of the signal and idler, which allows an un-ambiguous timing information retrieval. In particular, the timing information is extracted by measuring the power difference of two spectral slices, offset from the idler λ_I center wavelength, obtained by a narrow-band filter. Consequently, the sampling gate also acts as a precise phase detector. Finally, incorporating this phase detector into a phase locked loop (PLL), which controls the timing of the pump pulse, the sampling gate is precisely temporally locked to the input OTDM stream without any need for an external reference. The detailed experimental setup is shown in Fig. 12, whereas Fig. 13 shows

the performance test results of the parametric clock recovery in (i) a free-running mode (solid lines), and (ii) with the application of an outside 256 ps/s timing drift (dashed lines), putting a significant strain on the clock recovery capabilities. The realized parametric clock recovery proved fully resilient even under a strong outside disturbance over a wide range of data rates.

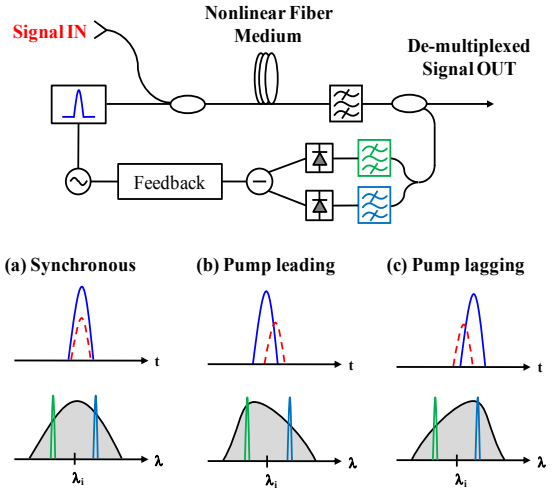

Figure 11. Self-phase tracked parametric sampling gate. Solid and dashed lines in temporal graphs denote pump and signal pulses respectively.

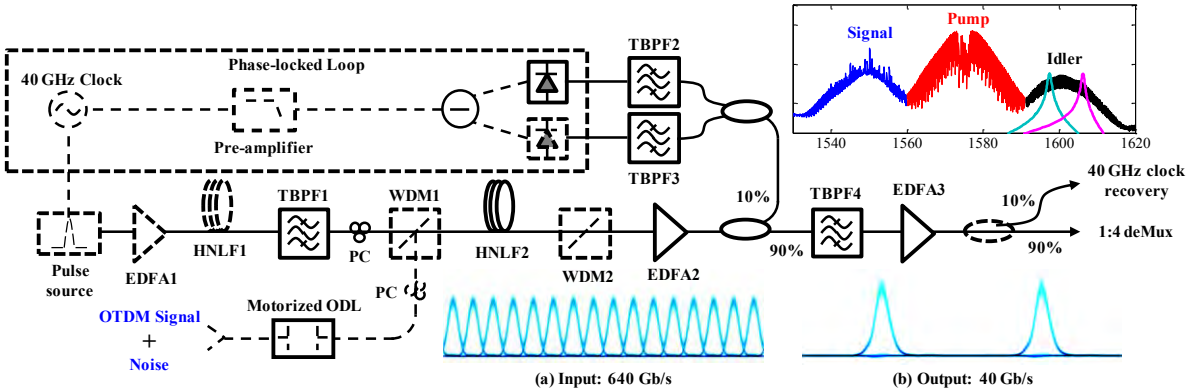

Figure 12. Experimental setup of the sampling gate. Inset shows the input 640 Gb/s and output 40 Gb/s eye diagrams, and the output spectrum of HNLF2. The transmission spectra of tuneable filters TBPF2 and TBPF3 are overlaid on the idler spectrum.

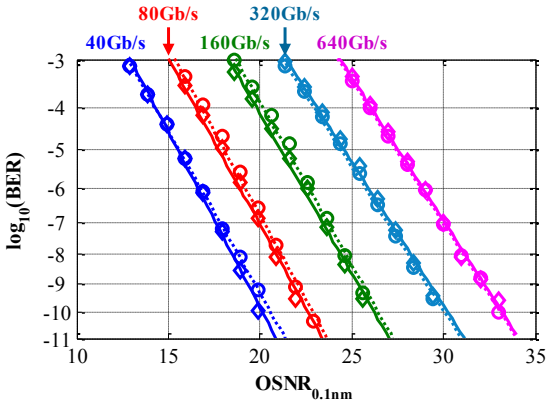

Figure 13. BER plots of de-multiplexed tributary at various input rates. Solid lines (diamond) and dashed lines (circle) denote BER measured without and with 256ps/s drift.

The described clock recovery was next used as a part of a fully self-contained 640 Gb/s receiver. The full schematic of the experiment is shown in the top of Fig. 14 and consists of two blocks, the 640 Gb/s transmitter and a 640 Gb/s OTD demux/receiver. Note that the two blocks are operated completely independently with two different clock sources. The cavity-less generated 40 GHz signal pulses had a width of 680 fs and a SNR of 33 dB. The pulses were modulated with data to create a 40 Gb/s stream with a quality (Q) parameter of 30 dB. After subsequent bit-rate multiplication, a high quality 640 Gb/s data stream was achieved having a wide-open eye with a Q of 26 dB. The receiver 40 GHz sub-rate sampling gate pulses had a width of 1.1 ps at the gate input. The optical spectrum of the sampling gate after HNLF4 is shown in the lower part of Fig. 14 with and without the 640 Gb/s data stream. The sampling pulses had an average power of 21.5 dBm at the input of the sampling fiber and the incoming frequency response of the used photo-detector. An eye-diagram of the tributary data captured by the optical input of a digital sampling oscilloscope after 2 nm bandpass filtering is shown as an inset in Fig. 14, which is of particular interest since it demonstrates an excellent operation of the phase tracking as well as the clock recovery.

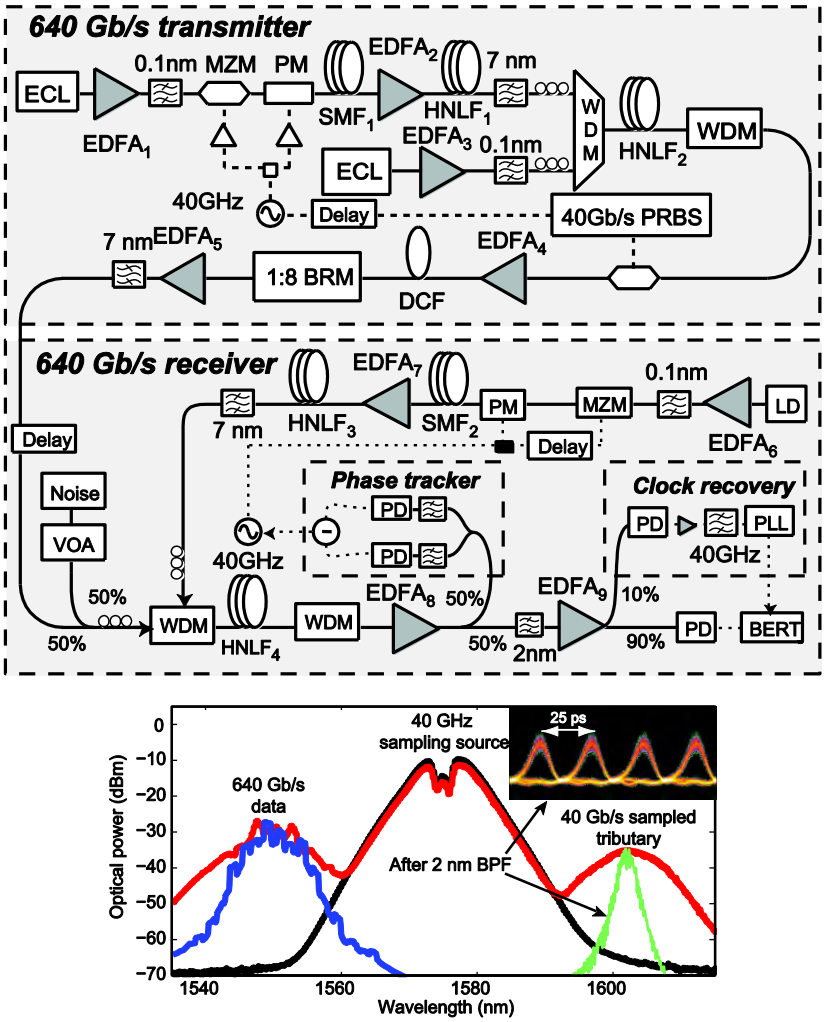

Figure 14. (top) The experimental setup consisting of 640 Gb/s generation and 640 Gb/s receiver. ECL: External cavity laser, MZM: Mach-Zehnder Modulator, PM: Phase modulator, WDM: wavelength division multiplexer, VOA: variable optical attenuator. (bottom) Optical spectra at the output sampling gate without and with 640 Gb/s data present, and the 40 Gb/s tributary after amplification and filtering with a 2 nm bandpass filter. The reference bandwidth is 1 nm. Inset: Eye diagram of the 40 Gb/s tributary after amplification and filtering with a 2 nm bandpass filter.

The operation of the 640 Gb/s transmitter and 640 Gb/s receiver was verified by rigorous bit error rate (BER) measurements of all the 16 tributaries in the aggregate high data rate channel. The performance was measured with respect to the OSNR, as explained in the previous section. A programmable optical delay in the incoming signal path was used to tune between the 16 tributaries of the 640 Gb/s data stream. The results are presented in Fig. 15, where the BER is plotted versus the OSNR, defined as total signal power divided by noise power measured with 0.1 nm resolution bandwidth with an OSA. The BER measurements of all 16 tributaries exhibit an error-free performance. The average BER of the 640 Gb/s channel is highlighted and the sensitivity, defined as the OSNR required to reach a BER of 10^{-9}, was 33.5 dB. Notably, this

value is very close to the practical limit of OSNR sensitivity at 33 dB. This outstanding performance is attributed to the basic properties of the parametric sampling gate.

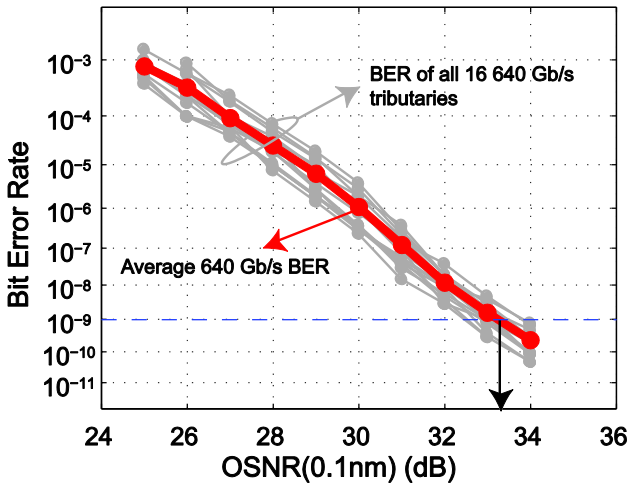

Figure 15. Bit error rate measurements of all sixteen 640 Gb/s tributary channels as function of OSNR at input of the sampling gate. The average BER of all channels are emphasized.

5) All-optical delays

The relentless demand for more information throughput over the past four decades has constantly instigated an increase in the capacity of communication links, as well as a thrust towards larger overall communication capacities. This trend inexorably led towards the evolution (deployment) of all-optical networks, sustained by the low loss and low cost of silica-based optical fibers. The necessary increases of transmission and processing speeds showed the first signs of electronic bottlenecks in the second half of the last decade. Indeed, since the late nineties, the necessary processing speeds of the electronics supporting optical transmission required the development of custom, application-specific boards and VLSI chips. In fact, this trend has continued ever since as the operating speeds continued to increase relentlessly.

Among the functionalities affected by the electronic bottleneck, all-optical delays were recognized early on as one of the key functionalities needed for an all-optical realization. All-optical delays are needed in a broad spectrum of underlying applications. Undeniably, all-optical delays are recognized as a key building block in: all-optical routing, optical correlation, high-speed gating, arbitrary waveform generation, beam-steering, optical coherence tomography and sensing applications. The aforementioned primary applications clearly imply the vital requirements for all-optical delays: (i) wavelength preservation, which in this respect implies that the out-put wavelength of the buffering element be the same as the input one, or, equivalently, that the delay be independent of the output wavelength and (ii) continuous tunability over the range of interest. Furthermore, the implied applications have for the last five years steered research into long – micro-second delays, capable of realizing 10000-bit (or more) delays at 10 Gb/s (or higher) speeds, irrespective of the output wavelength.

In this section, we present the first realization of the above long-lasting requirement. Microsecond delays are illustrated through two record experimental demonstrations: One at 10 Gb/s, for non-return-to-zero (NRZ) intensity-modulated signals, in addition to 40-Gb/s return-to-zero binary differential-phase-shift-keyed (RZ-DPSK) signals, validating the all-optical delay functionality for both currently deployed links, as well as those of the next generation.

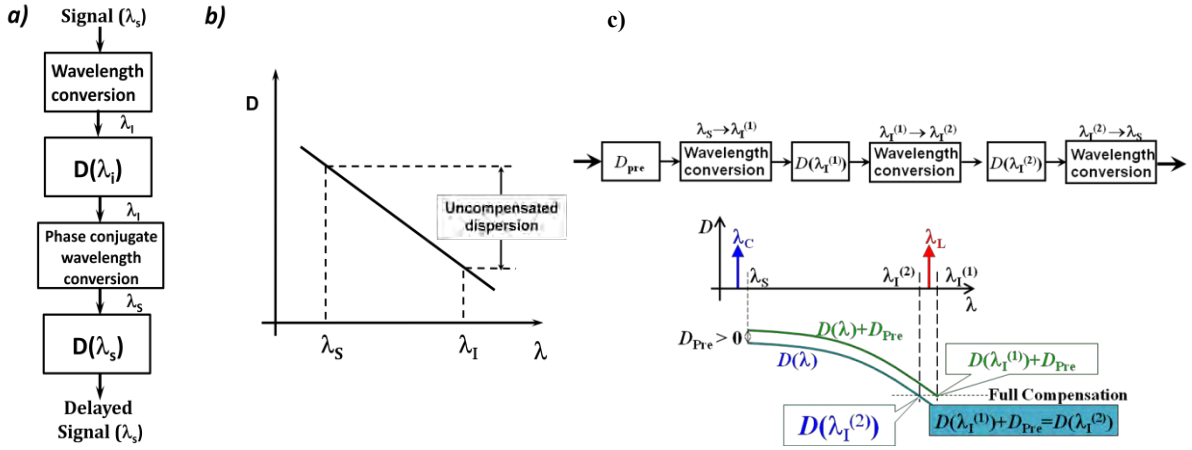

Figure 16. Two generations of all optical delay realizations based on wavelength conversion and dispersion: (a-b) delay with remnant accumulated dispersion used in demonstrations of 12 ns, 100ns, 400 ns and 700 ns delays; (c) delay concept with full second and third dispersion compensation, amenable to μs delays and high data-rates.

As is the case with other parts of this effort, optical delay realization has evolved through the different phases of the program. The fundamental concept schematics used are shown in Fig. 16. The first concept was used to demonstrate the delays from 12 ns to 700 ns [18-21], whereas the second one was used to demonstrate the previously ever-elusive micro-second delays [22, 23]. In particular, we shall concentrate on the ultimate micro-second demonstrations. The experimental setup used is shown in Fig. 17, whereas the delay dependence on the pump position is displayed in Fig. 18.

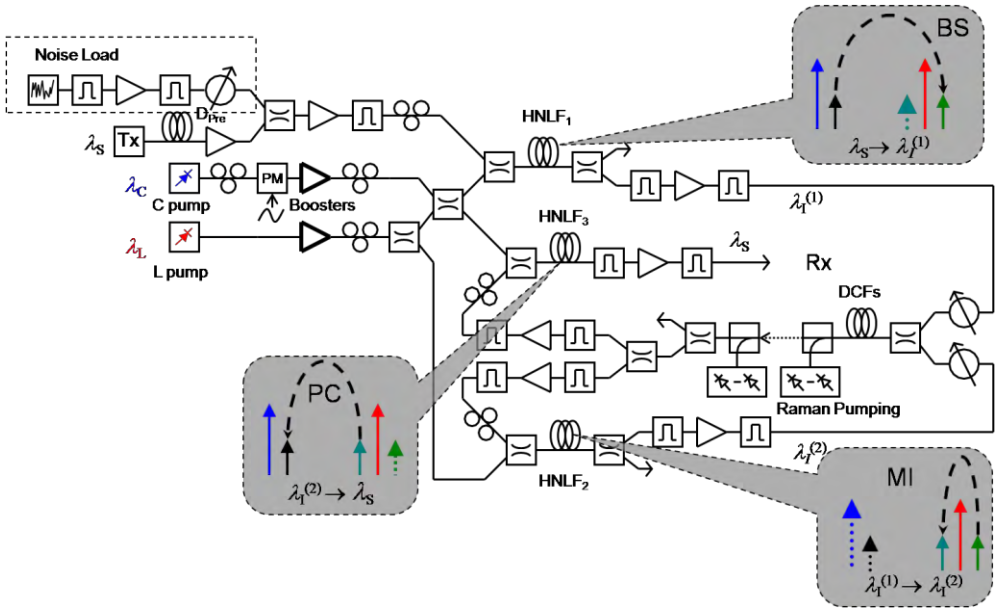

Figure 17. The μs delay experimental setup schematic. Three parametric conversions are used in succession in order to (i) achieve ms delay, and (ii) return the signal to the original wavelength, thus achieving a transparent delay element.

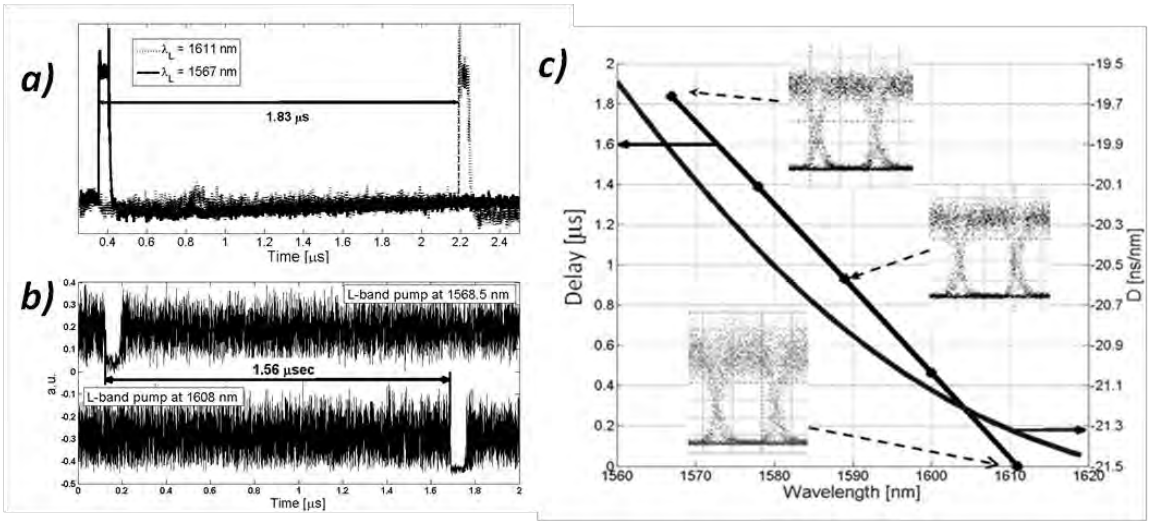

Figure 18. The μs delay demonstrations: (a) 10 Gb/s intensity modulated data; (b) 40 Gb/s phase modulated data; (c) delay dependence on the L-band pump position.

As noted previously, the most significant achievement in terms of all-optical delays within the POPS program is that not only μs delays have been demonstrated for the first time, but more importantly, delays capable of supporting high speed data have been implemented. Fig. 19 shows the integrity of the delayed information, as rigorously characterized in our experiments. As clearly demonstrated in Fig. 19, the executed parametric delays for the first time fully validate capability of a full support of high speed, modulation format independent data traffic, thus fully accomplishing the set program goals.

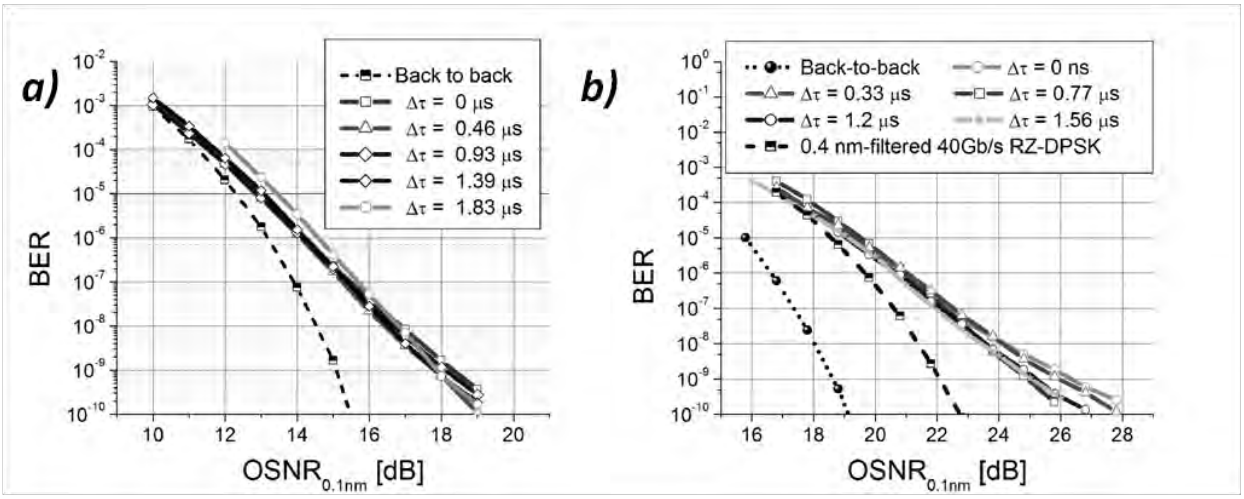

Figure 19. μs wavelength transparent delay high speed information support performance characterization.

6) Parametric Ultra Energy Efficient Transmission Penalty Reversal

Virtually all of the system demonstrations based on the MPASS architecture in the POPS project revolved around ultra high speed signal generation and detection. While definitely providing previously unavailable tools to signal characterization, detection and analysis, the final result, presented below, encompasses a full system demonstration from the signal generation, to transmission impairment erasure, and ultimately a successful reception of a THz signal. Indeed, although the need for high speed signal channels is recognized throughout the technological and DoD communities, the lack of means to attaining a successful manipulation and detection of the ultra-high speed signals is the main reason for the absence of such sophisticated systems in practice. The goal of the POPS program was in particular focused on obtaining the tools that would enable successful exploitation of high speed signals. Consequently, the following, first of its kind demonstration, reached an important milestone in high speed signal manipulation in that it displays not only the ability to interface THz information, but also to transport it over an appreciable distance. Indeed, ability to generate high speed information is useless for practical purposes without the ability to *transmit* and receive it at an acceptable level of quality. The precarious information conditioning at ever increasing speeds is precisely the reason why a THz channel has never been transmitted over distances longer than 20 km. After all, judging from the present state of the art, it is a difficult proposition for electronic circuits to come to a rescue in terms of digital signal processing at speeds higher than approximately 40 GHz. As a result, any means of mitigation of transmission impairments at these speeds necessarily needs to be all-optical.

Among the numerous impairments affecting signal propagation in single mode fibers, the dispersion plays by far the dominant role. The effect is easily explained from a physical perspective: a finite variation of the index of refraction in a single mode fiber, causes different frequencies to propagate at slightly different speeds. As a result, the information-bearing pulses spread and ultimately dispel, leading to a complete loss of information. The effect is, in fact, more severe with an increase of the underlying bandwidth. It is exactly this property that has made the transport of the THz signals prohibitively difficult to cope with. However, the key property of dispersive propagation is that of its self-cancellation with respect to time domain phase conjugation. Accordingly, finite bandwidth signals, after experiencing the amount of dispersion D, if subsequently subject to temporal phase conjugation (i.e. the reversal of the sign of the imaginary part of the optical field) will be fully restored if allowed to propagate through another span of a dispersive medium, equaling the dispersion (i.e. D) of the first dispersive line. In other words, after having been subject to phase conjugation, the acquired dispersion cancels, rather than adds up, and thus the concept of mid-span phase conjugation can be effectively used for signal restoration (i.e. the dispersion compensation) of signals of arbitrary rate.

In this experimental demonstration, two properties of parametric mixers have been used: (i) particular idlers in parametric conversion are exact phase-conjugate replicas of the input signal; (ii) momentum conservation in the case of a non-degenerate (two-pump) parametric device with cross-polarized pumps allows that the signal and idler coincide in frequency and yet be discernible by their state of polarization (thus providing a direct means to separate the frequency coinciding signal and idler) [24]. The process under consideration is illustrated in Fig. 20.

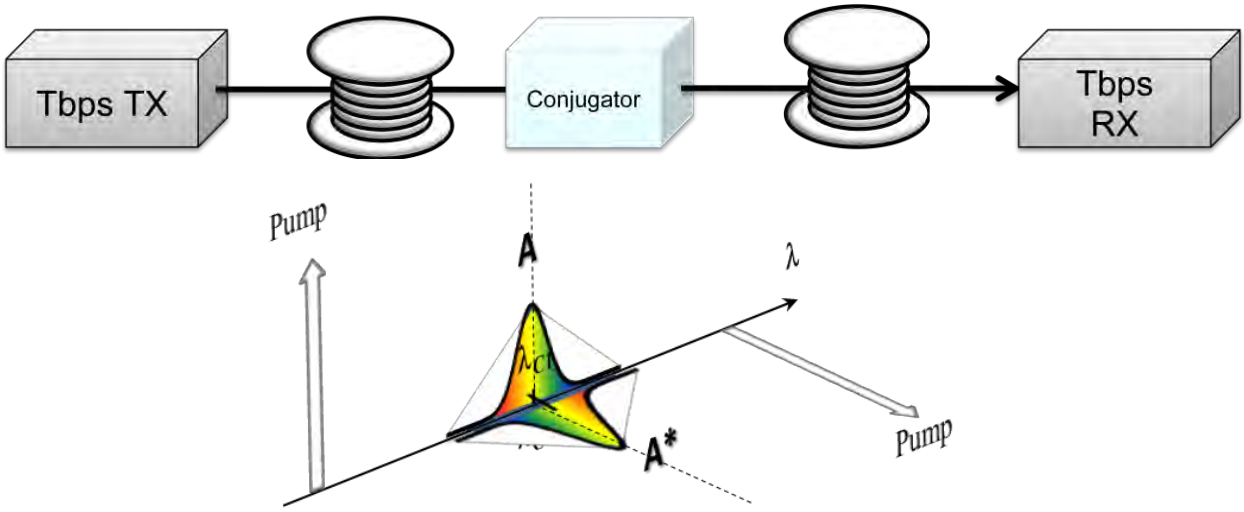

Figure 20. Mid-span phase conjugation transmission system. The conjugator element relies on a cross-polarized non-degenerate parametric amplifier concept, shown in the lower part of the figure.

The detailed experimental setup is shown in Fig. 21. The eye diagrams of the signal are shown at the transmit side and at the receiver, both with and without parametric penalty mitigation (i.e. the phase conjugation) on the left-hand-side of Fig. 22. As can be seen, the signals disintegrate within meters of propagation, whereas the received signal without parametric signal restoration is equivalent to a flat line with no information content. In sharp contrast, setting the parametric conjugator into the operational mode fully restores the signal even after 100 km of propagation. Finally, the quantitative characterization of the transmitted and the received signal is displayed in Fig. 22 (right). Note that errorless performance was measured after 100 km of propagation which surpasses all previous demonstrations by an order of magnitude. Furthermore, note that the level of signal integrity, as corresponding to the BER level of 10^{-9} outperforms all similar experiments performed so far, even at the speed of 100 Gb/s.

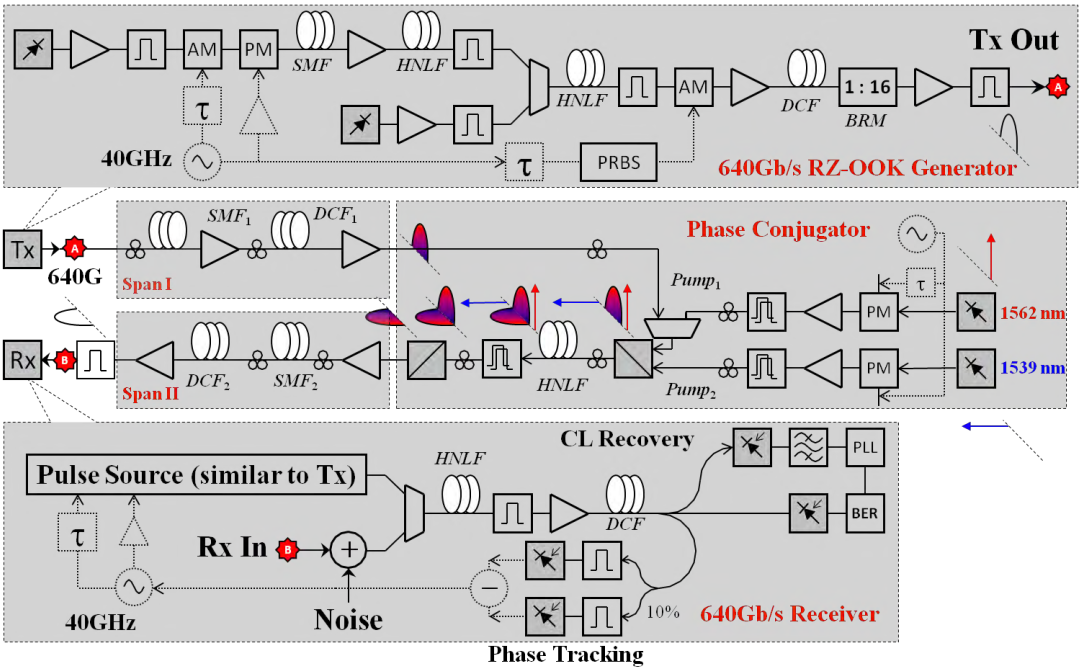

Figure 21. A detailed schematic of the experimental setup for the 100 km transmission experiment of THz signals. The three main components of the setup (transmitter, phase conjugator and parametric receiver) are presented in separate frames.

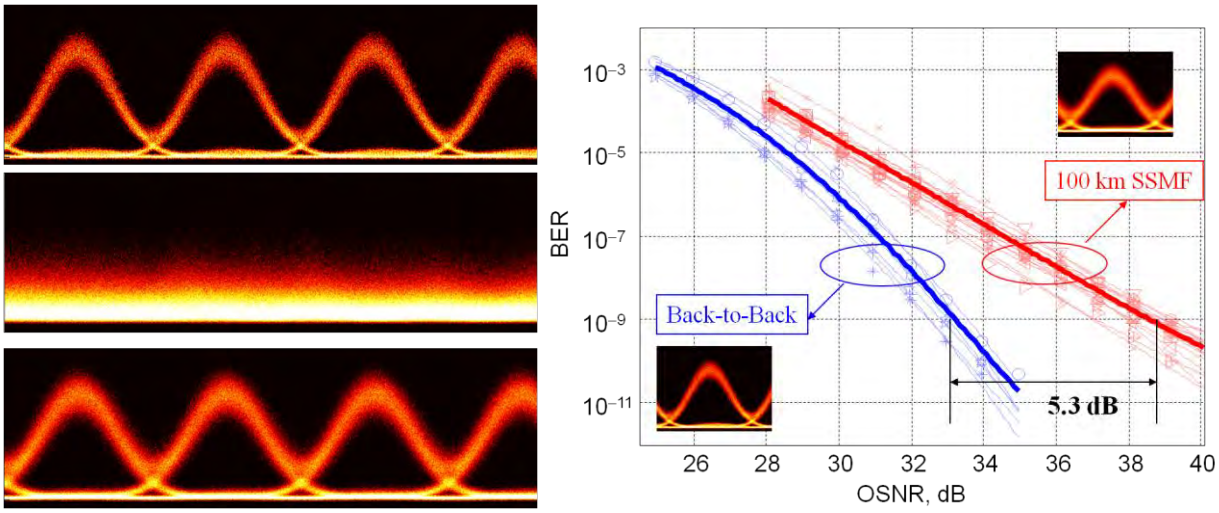

Figure 22. (left) 640 Gb/s signal eye diagrams at back-to-back (top), after 100 km propagation with no phase conjugation (middle), and with the application of a parametric phase conjugator (bottom). (Right) Measured performance at back-to-back and after 100 km propagation.

7) Summary

The Parametric Ultra Energy Efficient Transmission Penalty Reversal described in Section 6 succinctly displays the full success of the POPS program as it not only provided previously unattainable technology, but, more importantly, pushed the all-optical parametric concepts to a technological level that provides a complete THz signal manipulation from signal generation to successful transmission and error-free data detection. Indeed, the achievements of the POPS program span from (i) a new concept of a longitudinal nonlinear waveguide characterization, which resulted in the ability to repeatedly design unprecedented mixers surpassing 20 THz in bandwidth, and with a net positive continuous wave gain surpassing 20 dB, that is not available in any other nonlinear platform; (ii) ability to copy THz signals with impunity to tens of replicas; (iii) all-optical delays supporting high speed modulated data surpassing 1 μs; (iv) 10's of THz-fast all-optical sampling of signals; and lastly (v) an original fully scalable MPASS parametric processor for detection of THz signals availing access to all the (ultra high speed) data all the time. The achieved results are summarized in Table I. It ought to be emphasized that all of these superb achievements have been accomplished relying on the parametric mixing technology in optical fibers that was made possible through the DARPA visionary POPS program.

TABLE I: PROGRAM MILESTONES AND ACHIEVED RESULTS.

	Phase I (18 Months)	**Phase II (18 Months)**	**End of Phase II Result**
Parametric Bandwidth	>100 nm	>200nm	220nm
Multicaster Scaling	>8-fold	>16-fold	66-fold
Sampling Rate/Granularity	>320Gbps/8	>640Gbps/16	640 Gps/16
Delay Range	>500ns	>3500ns	1900ns*
Resolution / Jitter	1 ps / 300 fs	100 fs / 50 fs	50 / 50 fs

* Complemented by 640 Gbps transmission over 100 km and errorless reception.

8) References

[1] C.-S.Bres, N. Alic, A.H. Gnauck, R.M. Jopson, S. Radic, "Multicast Parametric Synchronous Sampling," IEEE Photon. Tech. Lett., Vol. 20, No. 14, pp. 1222 – 1224 (2008).

[2] S. Radic, "Parametric amplification and processing in optical fibers," Laser & Photonics Reviews, Vol. 2, pp. 498–513 (2008).

[3] Myslivets, N. Alic, S. Radic, "Spatially Resolved Measurement in Waveguides with Arbitrary Chromatic Dispersion" IEEE Photon. Technol. Lett. Vol. 20, No. 21, 1793 - 1795 (2008).

[4] E. Myslivets, N. Alic, J.R. Windmiller, S. Radic, "A New Class of High-Resolution Measurements of Arbitrary-Dispersion Fibers: Localization of Four-Photon Mixing Process," J. Lightwave Technol., Vol. 27, No. 3, 364 – 375 (2009).

[5] E. Myslivets, N. Alic, S. Radic, "Strict Localization of Nonlinear Interactions in Optical Fibers by Subsequent Brillouin Amplification and Attenuation" IEEE Photon Technol. Lett. Vol. 22, No. 3, pp. 170-172 (2010).

[6] E. Myslivets, N. Alic, S. Radic, "High Resolution Measurement of Arbitrary-Dispersion Fibers: Dispersion Map Reconstruction Techniques" J. Lightwave Technol., Vol. 28, No. 23, pp. 3478-3487 (2010).

[7] S. Moro, E. Myslivets, J.R. Windmiller, N. Alic, J.M. Chavez Boggio, S. Radic "Synthesis of Equalized Broadband Parametric Gain by Localized Dispersion Mapping" IEEE Photonics Technology Letters, Vol. 20, No. 23, pp. 1971 – 1973 (2008).

[8] J.C. Boggio, S. Moro, E. Myslivets, J.R. Windmiller, N. Alic, S. Radic "155-nm Continuous-Wave Two-Pump Parametric Amplification" IEEE Photon. Technol. Lett. Vol. 21 No. 10, pp. 612-614 (2009).

[9] C.S. Bres, J.M. Chavez-Boggio, N. Alic, S. Radic, "1-to-40 10-Gb/s Channel Multicasting and Amplification in Wideband Parametric Amplifier," IEEE Photon. Technol. Lett., Vol. 20, No. 16, pp. 1417 – 1419 (2008).

[10] C.-S. Brès, A.O.J. Wiberg, J. Coles, S. Radic " 160-Gb/s optical time division multiplexing and multicasting in parametric amplifiers," Optics Express, Vol. 16, No. 21, pp. 16609-16615, (2008).

[11] C.S. Bres, N. Alic, E. Myslivets, S. Radic, "Scalable Multicasting in One-Pump Parametric Amplifier" J. Lightwave Technol., Vol. 27, No. 3, 356 - 363 (2009).

[12] C.-S. Bres, A.O.J. Wiberg, B.P-.P. Kuo, N. Alic, S. Radic " Wavelength Multicasting of 320-Gb/s Channel in Self-Seeded Parametric Amplifier" IEEE Photon. Technol. Lett. Vol. 21, No. 14, pp. 1002-1004 (2009).

[13] A.O.J. Wiberg, C.S. Bres, B.P.P. Kuo, J.X. Zhao, N. Alic, S. Radic, " Sampling of Multiple 320-Gb/s Channels by Single Parametric Gate " IEEE Photon. Technol. Lett. Vol. 21, No. 12, pp. 796-798 (2009).

[14] A.O.J. Wiberg, C.S Bres, B.P.-P. Kuo, J.M.C. Boggio, N. Alic, S. Radic, "Multicast Parametric Synchronous Sampling of 320-Gb/s Return-to-Zero Signal" IEEE Photon. Technol. Lett. Vol. 21, No. 21, pp. 1612-1614 (2009).

[15] C.S. Bres, A.O.J. Wiberg, B.P.-P. Kuo, J.M. Chavez-Boggio, C.F. Marki, N. Alic, S. Radic, S."Optical Demultiplexing of 320 Gb/s to 8 40 Gb/s in Single Parametric Gate" J. Ligthwave Technol. Vol 24, No. 4, pp. 434-442 (2010).

[16] A.O.J. Wiberg, C.S. Bres, B.P.P. Kuo, J.X. Zhao, N. Alic, S. Radic, "Pedestal-Free Pulse Source for High Data Rate Optical Time-Division Multiplexing Based on Fiber-Optical Parametric Processes" IEEE J. Quantum Electronics, Vol. 45, No. 11, pp. 1325-1330 (2009).

[17] B.P.-P. Kuo, AO.J. Wiberg, C.-S. Brès, N. Alic, S. Radic " Ultrafast Clock Recovery and Sampling by Single Parametric Device," IEEE Photon. Technol. Lett., Vol. 23, No. 3, pp. 191-193,(2011).

[18] N. Alic, J.R. Windmiller, J.B. Coles, S. Moro, E. Myslivets, R.E. Saperstein, J.M. Chavez Boggio, C.S. Bres and S. Radic, "105ns Continuously Tunable Delay of 10Gbps Optical Signal" IEEE Photonics Technology Letters, Vol. 20, No. 13, pp. 1222-1224 (2008).

[19] N. Alic, J.R. Windmiller, J.B. Coles, S. Radic, "Two Pump Parametric Delays" IEEE Journal on Selected Topics in Quantum Electronics, Vol. 14, No. 3, pp. 681-690 (2008).

[20] E. Myslivets, N. Alic, J.R. Windmiller, R.M. Jopson, S. Radic, S, "400-ns Continuously Tunable Delay of 10-Gb/s Intensity Modulated Optical Signal," IEEE Photon. Technol. Lett., Vol. 21, No. 4, 251 – 253 (2009).

[21] S. Moro, E. Myslivets, N. Alic, J.X. Zhao, A.J. Anderson, J.M. Aparicio, J.B. Coles, J.M. Chavez Boggio, S. Radic "720-ns Continuously Tunable Parametric Delay of a 10-Gb/s Optical Signal" IEEE Photon. Technol. Lett. Vol. 21, No. (2009).

[22] N. Alic, E. Myslivets, S. Moro, B.P.-P. Kuo, R.M. Jopson, C.J. McKinstrie, S. Radic, "Microsecond Parametric Optical Delays" J. Lightwave Techol. Vol. 28, No. 4, pp. 448-455 (2010).

[23] E. Myslivets, N. Alic, S. Moro, B.P.P. Kuo, R. M. Jopson, C. J. McKinstrie, M. Karlsson, and S. Radic, "1.56-μs continuously tunable parametric delay line for a 40-Gb/s signal," Opt. Express 17, 11958-11964 (2009).

[24] B.P.-P. Kuo, E. Myslivets, A.O.J. Wiberg, S. Zlatanovic, C.S. Bres, S. Moro, F. Gholami, A. Peric, N. Alic, S. Radic, "Transmission of 640-Gb/s RZ-OOK Channel Over 100-km SSMF by Wavelength-Transparent Conjugation" J. Ligthwave Technol. Vol. 29, No. 4, pp. 516 - 523 (2011).